ABSTRACT

HEAT CAPACITY OF $CuSiO_3 \cdot H_2O$ FROM $2^{\circ}K$ TO $40^{\circ}K$

by Warren Rice Eisenberg

The heat capacity of $CuSiO_3 \cdot H_2O$ was measured in an attempt to find evidence for a magnetic transition in the temperature range of $2^{\circ}K$ to $40^{\circ}K$. Such a transition was observed and was characterized by an anomaly at $21^{\circ}K$ in the specific heat vs. temperature curve.

The anomalous behavior may be attributed to the fact that spins of the magnetic ions go from random orientations in the paramagnetic state to an antiparallel alignment in the antiferromagnetic state. The magnetic contribution to the specific heat was found to be superimposed on the normal lattice curve as predicted in the theories of Van Vleck and Debye.

HEAT CAPACITY OF $CuSiO_3 \cdot H_2O$ FROM $2^{\circ}K$ TO $40^{\circ}K$

By

Warren Rice Eisenberg

A THESIS

Submitted to
Michigan State University
in partial fulfillment of the requirements
for the degree of

MASTER OF SCIENCE

Department of Physics and Astronomy

1963

ACKNOWLEDGMENTS

The author wishes to express his gratitude to Dr. H. Forstat whose guidance and suggestions made this research possible. His many hours of assistance are truly appreciated.

The author also wishes to thank Mr. N. Love for his help in assisting with the experimental operations and the United States Air Force Office of Scientific Research for financially supporting this project.

* * * * *

TABLE OF CONTENTS

LIST OF FIGURES

THEORY

The Basic Equation for Heat Capacity Studies.

The mean heat capacity is defined[1] as the ratio of a given amount of heat put into a substance divided by the corresponding change in temperature of the substance, or

$$\bar{C} = \frac{\Delta Q}{\Delta T} . \qquad (1)$$

Frequently (especially at low temperatures) $\bar{C}$ exhibits a strong temperature dependence, and thus the true heat capacity is given as

$$C = \lim_{\Delta T \to 0} \frac{\Delta Q}{\Delta T} = \frac{dQ}{dT} . \qquad (2)$$

Experimentally one must hold the pressure or volume of the substance constant while making the heat capacity measurement; furthermore, the heat capacity per unit mass or mole (specific heat) is of importance. Thus the definition is further refined so that

$$\frac{C_v}{m} = c_v = \frac{\left(\frac{dQ}{dT}\right)_v}{m} , \qquad (3)$$

where the small "c" indicates specific heat capacity, and the subscript "v" indicates that the volume is to be held constant; m denotes mass or moles.

Many of the theoretical discussions on specific heat capacities are based on energy relations. To see why one needs only to consider

energies use is made of the First Law of Thermodynamics:

$$dQ = dU + pdV. \tag{4}$$

Assume that $U = f(T, V)$. Then

$$c_v = \left(\frac{\partial U}{\partial T}\right)_v . \tag{5}$$

Equation (5) indicates a simple relation showing that if there eixists an expression giving the internal energy of a substance as a function of temperature, one differentiates with respect to the temperature, keeping the volume constant, to find the heat capacity. Experimentally, however, it is quite difficult to hold a substance at a constant volume while performing measurements at different temperatures. It is much easier to keep the pressure constant while making heat capacity measurements. If one assumes $U = f(T, P)$, the result obtained using Equation (4) is

$$c_p = \left(\frac{\partial U}{\partial T}\right)_p + p\left(\frac{\partial v}{\partial T}\right)_p . \tag{6}$$

Equation (6) obviously would be much more difficult to work with theoretically. Fortunately, however, as the temperature approaches low values c_p and c_v are practically equal. This fact is expressed in the equation $c_p - c_v = \frac{\beta^2 vT}{\kappa}$, [2] where β is the coefficient of volume expansion, and κ is the isothermal compressibility. Thus Equation (5) is used for theoretical discussions while experimentally the pressure is held constant. Equation (5), then, is a basic equation for heat capacity studies.

Classical Theory of Specific Heats.

The question now arises as to what exactly contributes to the internal energy of a solid; more precisely, if one can find an expression for U as a function of T, then one needs merely to insert this into Equation (5) to find an expression for the specific heat of a solid.

Consider first a non-metallic substance. Here it can be assumed that the electrons act in unison with the atoms.[3] The important contribution to the internal energy comes from the vibrational energy of each atom in the solid. Classical mechanics predicts that the vibrational energy of each atom can be represented by the energy of three harmonic oscillators. Each oscillator will have a potential energy equal to $1/2kT$ and a kinetic energy equal to $1/2kT$, where k is Boltzman's constant. Hence each atom contributes $3kT$ to the solid's energy. If exactly one mole of the substance is considered, then there will be N_o (Avogadro's number) atoms, and the molar specific heat will be (using Equation (5))

$$c_v = 3R, \tag{7}$$

where $R = N_o k$ is the gas constant. Equation (7) is referred to as the Law of Dulong and Petit. It is found that many solids do have a specific heat of 3R, but only at high temperatures. The above relation is not valid at the lower temperature region.

In the case of metallic substances one can assume that the electrons

behave as an "electron gas." Drude[4] postulated that a metal consists of positive metal ions whose valence electrons are free to move between the ions as if they constituted an electron gas, and the electrons are free to move throughout the entire crystal subject only to the laws of classical mechanics. Classical theory states that the average kinetic energy in a monatomic gas is 3/2 kT per atom. The average energy per mole then becomes $3/2\ N_o kT = 3/2\ RT$. The specific heat contribution of electrons is therefore given by

$$c_v = 3/2\ R. \tag{8}$$

Thus in the case of metals the total specific heat capacity is the sum of Equations (7) and (8).[5] This gives $c_v = 9/2\,R$. It is observed that the specific heats of metals tend to be more in agreement with Equation (7) at high temperatures rather than 9R/2 and, furthermore, that Equation (8) is invalid for low temperature electronic contributions.

Quantum Mechanical Theory of Specific Heats.

A typical graph of c_v vs. T for most substances appears as shown in Figure 1, here shown for aluminum.[6] At the higher temperatures there is an asymptotic approach to the classically predicted value of 3R, as given in Equation (7). At the lower temperatures, however, $c_v \propto T^3$. In an attempt to explain experimental results similar to Figure 1, Einstein[7] postulated that the atoms of a crystal oscillate independently and with the same frequency ν: A crystal containing N atoms can be

represented by 3N harmonic oscillators all vibrating with frequency ν. If one mole of the substance in question is considered ($N = N_o$) and use is made of quantum mechanics, the energy becomes $U = 3N_o h\nu/[\exp(h\nu/kT) - 1]$, where h is Planck's constant. The specific heat is again obtained by substitution of U into Equation (5); the result is

$$c_v = 3R \left(\frac{h\nu}{kT}\right)^2 \frac{\exp(h\nu/kT)}{[\exp(h\nu/kT) - 1]^2}. \tag{9}$$

A plot of Equation (9) shows a graph similar to Figure 1 but does not coincide with it. Einstein's equation shows fairly good agreement with experiment only in the range $c_v > 3R/2$.[8]

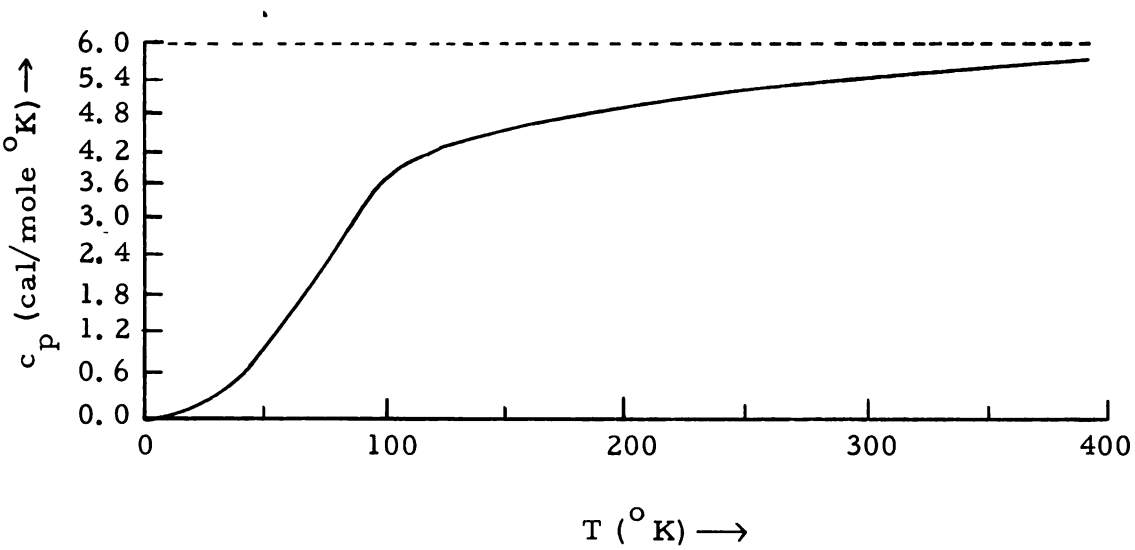

FIGURE 1. The specific heat of aluminum.

Consequently Debye used a model of a crystal in which he related the specific heat to the elastic properties of the solid. Using Boltzman's Theorem and quantum mechanics it is found that the energy of an assembly of oscillators having a continuous frequency distribution is given by

$$U = kT\int_{0}^{\nu_m} (h\nu/2kT + \frac{h\nu/kT}{\exp(h\nu/kT) - 1})q(\nu)\, d\nu, \tag{10}$$

where $q(\nu)d\nu$ is the number of oscillators in the frequency range from ν to $\nu + d\nu$, and ν_m is the maximum frequency of any oscillator. One major difficulty in using Equation (10) is the determination of $q(\nu)$. In an attempt to find this distribution Debye assumed that, contrary to the theory of Einstein, the atoms in a solid do not vibrate independently.

Debye's solution to the theory of specific heats involves the determination of the normal modes of vibration of a continuous solid made up of individual atoms. The frequencies of vibration are quantized according to

$$\nu = \frac{v}{2}\sqrt{\left(\frac{n_x}{L_x}\right)^2 + \left(\frac{n_y}{L_y}\right)^2 + \left(\frac{n_z}{L_z}\right)^2}\ , \tag{11}$$

where v is the velocity of propagation and n_x, n_y, n_z are integers in the direction of the three axes of length L_x, L_y, L_z. The quantity under the root can be thought of as a radius vector R:

$$\nu = \frac{v}{2} R. \tag{12}$$

The number of allowed frequencies dN lying in a shell between R and (R + dR) is $4\pi R^2 dR$. Only positive integers are allowed; thus one considers only points in the positive octant of the shell. This gives $1/8\ (4\pi R^2 dR)$, or from Equation (12), $4\pi\nu^2 d\nu/v^3$. Each lattice point has a unit volume associated with it that contains V allowed frequencies. Therefore, the total number of allowed frequencies in the range $d\nu$ is

$$dN = \frac{4\pi\nu^2 d\nu}{v^3}\ V. \tag{13}$$

If three mutually orthogonal directions of vibration are considered, one longitudinal and two transverse, Equation (13) becomes

$$dN = 4\pi\nu^2 d\nu\ V\left(\frac{1}{v_l^3} + \frac{2}{v_t^3}\right). \tag{14}$$

$\frac{dN}{d\nu}$ is $q(\nu)$ in Equation (10). Debye assumed that there existed a certain cutoff frequency ν_m and showed that Equation (10) takes on the form

$$U = \frac{9Nh}{\nu_m^3}\int_0^{\nu_m} \frac{\nu^3 d\nu}{\exp(h\nu/kT) - 1}. \tag{15}$$

In his final result Debye defined a characteristic temperature $\theta_D = h\nu_m/k$ and showed by numerical integration that for $T << \theta_D$ the specific heat is given by

$$c_v = aT^3, \tag{16}$$

where $\alpha = 12\pi^4 R/5\theta_D^3$. Equation (16) is the universally famous Third Power Law of Debye. Debye's results are in good agreement with experimental work at both high and low temperatures.

One other important quantum mechanical result is the specific heat contribution of free electrons at low temperatures. Making use of the Pauli Exclusion Principle it is found that the electronic contribution is given by

$$c_v = \beta T, \tag{17}$$

where β is a constant. Thus in the most general discussion of specific heats at low temperatures the sum of Equations (16) and (17) expresses c_v as a function of T:

$$c_v = \alpha T^3 + \beta T. \tag{18}$$

Paramagnetic-Antiferromagnetic Transitions.

Instead of indicating a c_v vs. T curve exactly as shown in Figure 1, many substances exhibit a curve like that in Figure 2, here shown for

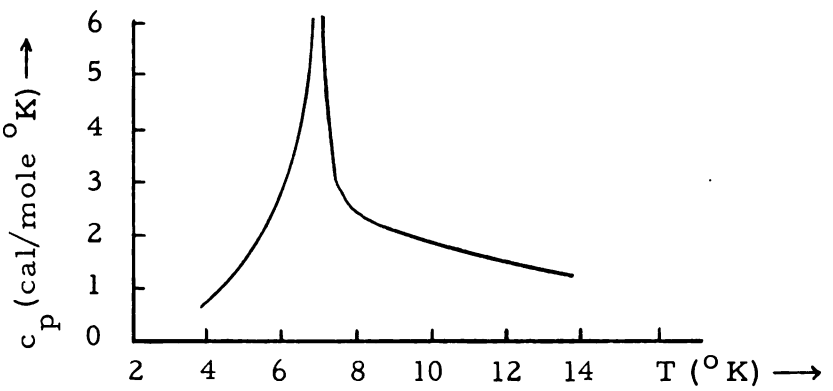

FIGURE 2. Specific heat of $NiBr_2 \cdot 6H_2O$.

the specific case of $NiBr_2 \cdot 6H_2O$.[10] The striking feature here is the appearance of an anomalous peak. Notice that the temperature range plotted here is small in comparison to Figure 1 and that actually the peak in Figure 2 would appear as a well defined kink superimposed on Figure 1 at the indicated temperature. λ-shaped curves like the above are characterized by a maximum value at the temperature indicated by T_N, the Neél temperature.

What is happening to the internal energy of certain solids to give rise to a curve such as Figure 2? In answering this question reference will be made to two important papers by Van Vleck.[11, 12]

Basically the situation is most easily explained by stating that when $T > T_N$ the substance is in a paramagnetic state and when $T < T_N$ the substance is in an antiferromagnetic state. A brief discussion will point out what is meant by paramagnetism and antiferromagnetism. When matter is placed in a magnetic field, magnetic forces on the moving electrons cause some type of reorientation of electron orbits in the atoms so that the substance itself will set up a macroscopic field. A paramagnetic substance is characterized by an extremely small field proportional to and in the direction of the external field. Antiferromagnetic substances are characterized by antiparallel spin moments (ordered spins) in adjacent atoms, thus producing no field. Furthermore, paramagnetic substances are characterized by random spin moments (disordered spins) of the atoms.

Figures 3, 4, and 5 show some experimental work done in Leiden, Holland on the antiferromagnetic properties of $CuCl_2 \cdot 2H_2O$[13] and will help to explain the theoretical results of Van Vleck more clearly. Figure 3 shows the dependence of the magnetic field in the crystal on

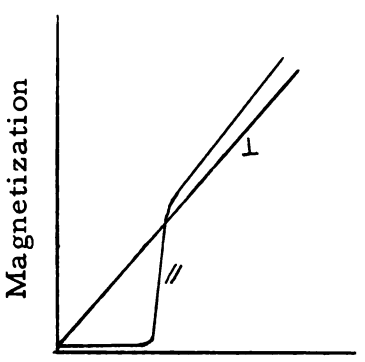

External Field

FIGURE 3

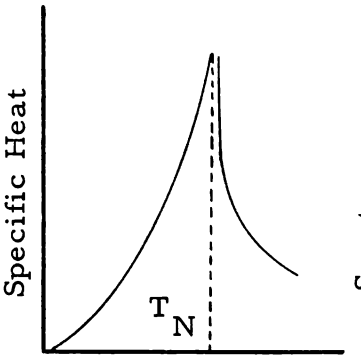

Temperature

FIGURE 4

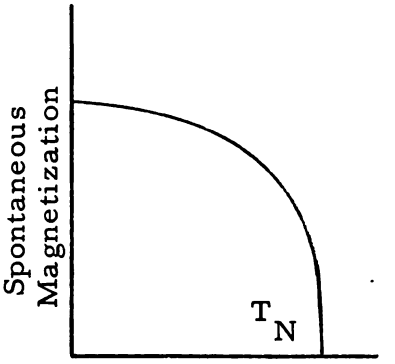

Temperature

FIGURE 5

the applied field parallel and normal to the preferred direction. While the magnetization at right angles shows no anomaly, the parallel one remains small at low fields and then rises abruptly to become eventually proportional to the applied field. This suggests the behavior of a critical (threshold) field in addition to critical temperature. The latter is clearly marked in the specific heat (Figure 4) indicating the disappearance with rising temperature of long range order. That the specific heat decreases only gradually to its normal value above the critical temperature means that some short range order evidently persists

above T_N. The spontaneous magnetization (Figure 5) vanishes at $T = T_N$, the same place at which the specific heat shows an anomaly. Furthermore, magnetic susceptibility curves with kinks in them are frequently found.[14] Any good theory on anomalous specific heats, then, should simultaneously satisfy all of these observations.

In deriving results for the paramagnetic part of curves like Figure 2, Van Vleck considered the influence of dipole-dipole coupling. Here the partition function Z of an ensemble of atoms is determined assuming each atom has a magnetic moment and is subject to the exchange coupling with the moments of other atoms. Use is made of the statistical mechanics relation showing c_v as a function of T:

$$c_v = \frac{\partial}{\partial T}\left(kT^2 \frac{\partial \ln Z}{\partial T}\right). \tag{19}$$

To find Z the Hamiltonian is expressed as

$$H = \sum_{j>i} \frac{1}{r_{ij}^3}\left[\bar{\mu}i \cdot \bar{\mu}j - \frac{3(\bar{\mu}_i \cdot \bar{r}_{ij})(\bar{\mu}_j \cdot \bar{r}_{ij})}{r_{ij}^2}\right], \tag{20}$$

where $\bar{\mu}_i$ is the magnetic moment of atom i and $\bar{r}_{ij}$ the radius vector connecting atoms i and j. Use of Equations (19) and (20) in conjunction with the fact that $Z = \sum_\lambda \exp(-W_\lambda/kT)$, where the sum is over all the energy states of the crystal and W_λ are the characteristic values of the Hamiltonian, eventually leads to the result

$$c_v = \frac{\gamma}{T^2}, \tag{21}$$

where γ is a characteristic constant. Thus the total heat capacity in the paramagnetic state is the sum of Equations (18) and (21) or

$$c_v = \alpha T^3 + \beta T + \frac{\gamma}{T^2}. \tag{22}$$

In the antiferromagnetic state there is, as yet, no simple relation between c_v and T. Consider the atoms of a crystal to be arranged on two interpenetrating sublattices so that the spin moments of atoms in one sublattice array A have an opposite sense to the other sublattice array B; furthermore, assume the nearest neighbors in A are contained entirely in B as shown in Figure 6. Thus when one considers exchange interactions of an atom in A, only effects produced by the atoms in B need to be taken into account. The effective potential to which an atom i is subjected is given by

$$V_i = -2J\bar{S}_i \cdot \sum_j \langle \bar{S}_j \rangle, \tag{23}$$

where $\bar{S}_i$ is the spin angular momentum vector of atom i, $\bar{S}_j$ is the spin

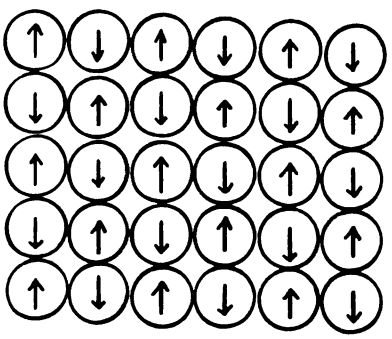

FIGURE 6. Antiferromagnetic spin moments.

angular momentum vector of atom j, and J is the exchange integral. By considering the effect of various external field orientations on the spin vectors, the problem reduces to one of scalar functions. If <S> denotes the mean value of all the spins in sublattice A, then the mean value of all the spins in sublattice B is also given by <S>; let s denote the spin quantum number (i.e. $\frac{1}{2}$, $\frac{3}{2}$, $\frac{5}{2}$, . . .). An important result is

$$<S> = sB_s(y_o), \tag{24}$$

where

$$B_s(y) = \frac{2s+1}{2s} \coth\left(\frac{2sy+y}{2s}\right) - \frac{1}{2s} \coth\left(\frac{y}{2s}\right) \tag{25}$$

is the Brillouin function and

$$y_o = \frac{2|J|zs <S>}{kT}, \tag{26}$$

z being the number of neighbors possessed by a given atom. The solution <S> of Equation (24) is s as $T \rightarrow 0$; at $T = T_N$ <S> = 0, showing the complete antiparallel arrangement of the spins. The Neél temperature T_N is given by

$$T_N = \frac{2}{3}|J|\frac{z}{k} s(s+1). \tag{27}$$

A plot of Equation (24) for the case $s = \frac{1}{2}$ is shown in Figure 7.[15] Note the agreement with Figure 5. If N denotes the number of atoms per unit volume then

$$c_v = -2N|J|z <S> \frac{d<S>}{dT}. \tag{28}$$

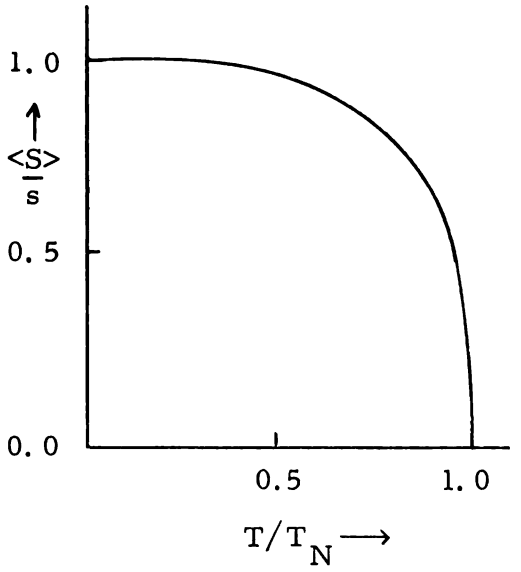

FIGURE 7.

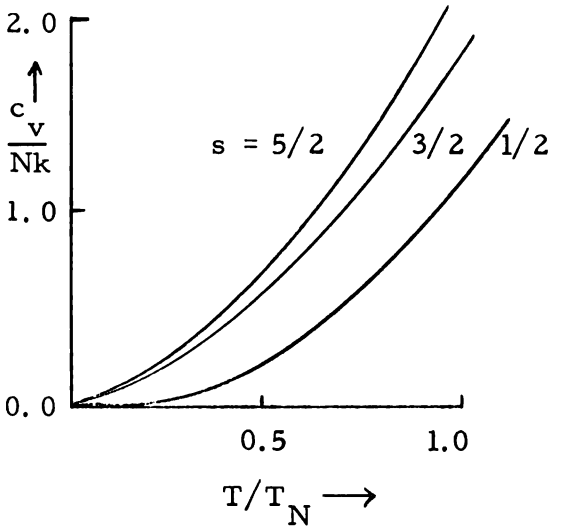

FIGURE 8.

A plot of Equation (28) is given in Figure 8.[16] Here note the resemblance to Figures 2 and 4 for $T < T_N$.

Suffice it to say that Van Vleck's theory does satisfy all of the aforementioned diagrams and physical anomalies; thus it can be said that in the case of a paramagnetic-antiferromagnetic transition magnetic contributions strongly affect the internal energy.

Entropy Considerations.

It is possible to obtain some idea of the amount of disorder-order involved in a paramagnetic-antiferromagnetic transition by considering entropy changes.[17, 18] Above the Neél temperature Equation (22) yields

$$c_v T^2 = \alpha T^5 + \gamma, \tag{29}$$

for the case of a non-metal where the electronic contribution is negligible. A plot of $c_v T^2$ vs. T^5 will give a straight line, the slope of

which is α and the intercept of which is γ; frequently α turns out to be quite small and γ comparatively large. For $T > T_N$ Equation (21) can now be used to calculate the entropy S due to magnetic contributions:

$$S = \int_{T_1}^{T_2} \frac{c_v}{T} dT = \gamma \int_{T_N}^{\infty} \frac{dT}{T^3} \tag{30}$$

Below the Neél temperature one must resort to graphical methods to find S due to magnetic contributions. First the low temperature end of the c_v vs. T curve is extrapolated to T = 0. Then the T^3 lattice contribution to the specific heat is calculated from Equation (16). α is found by measuring the slope of the graph obtained by plotting Equation (29). The lattice contribution is subtracted from the total specific heat capacity curve. The resulting values are the magnetic contribution to the specific heat, C_{mag}. A graph of C_{mag}/T vs. T is now plotted and the area of the resulting curve measured. As is indicated by the first part of Equation (30) the area measurement will provide the entropy of the antiferromagnetic state. The total magnetic contribution to the entropy is given by the expression

$$S = R \ln (2s + 1), \tag{31}$$

and thus the experimental results may be compared with theory.

EXPERIMENT

Crystal Preparation.

In order to experimentally measure specific heats it was necessary to use a modified form of Equation (3), or $\Delta Q = mc_v \Delta T$. A known amount of heat ΔQ was put into a crystal of mass m and the resulting temperature change ΔT measured.

The crystal to be examined was wrapped with a manganin heater wire enabling known amounts of heat to enter the crystal. A carbon resistor was inserted in the crystal for temperature measurements.[19] A small amount of Glyptal was used to fasten the wire and resistor in place. Connections to the calorimeter leads were made by small lengths (6 inches) of teflon wire. The carbon resistance thermometer (thermistor) had a room temperature resistance of 56 ohms. The heater wire resistance was about 150 ohms.

The particular crystal used in this experiment was dioptase, or $CuSiO_3 \cdot H_2O$, a mineral mined in S. W. Africa. Difficulty had previously been encountered with this crystal[20] in that it showed an apparent inability to retain heat put into it with the experimental setup used. One cause of this was believed to be a possible outgassing of the crystal creating an undesirable exchange gas. This would make thermal isolation of the crystal, a necessary procedure for measuring heat capacities, impossible. Thus a very small can composed of copper

and low melting solder was constructed around the crystal (Figure 9) to prevent the crystal from outgassing. Originally the experiment was carried through without the special container; difficulty was again

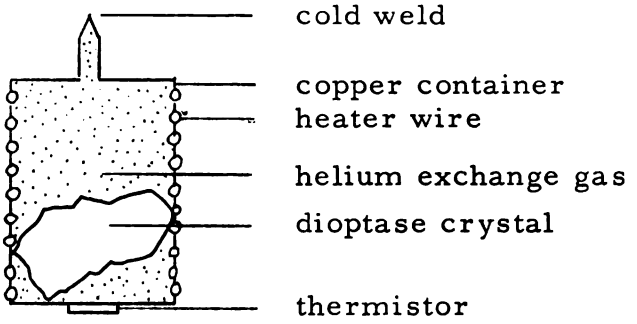

FIGURE 9. Dioptase and copper container.

encountered. Thus a slight modification was made on the wiring: The heater wire was wrapped around the container containing the crystal and the thermistor placed into contact with the container. Glyptal was again used as a fastener. The can was evacuated and helium exchange gas at 1 mm Hg pressure inserted to insure good thermal contact between the crystal and copper-solder container. A cold welding pliers was used to seal off the low pressure helium from the atmosphere. A small amount of solder was then placed over the weld to be certain that no leakage would occur when in the lower temperature region. The heat capacity of the entire setup was thus measured. Later the can was disassembled and the crystal removed; the can was then bathed in acetone so that no possible contamination resulted from fragments of

the dioptase. The can was reassembled and a heat capacity measurement made on it. From these data (given in the Appendix) the specific heat as a function of temperature was obtained.

Calorimeter Design.

Nuclear magnetic measurements[21] indicated a possible transition point (i. e. Neél temperature) to be around 21° K. Thus a calorimeter was designed which would permit temperature measurements from liquid helium temperatures (1.2° to 4.2° K) to about 70° K. The calorimeter consisted of three brass cans, generally described as small, medium, and large; it is shown diagramatically in a one to one scale in Figure 10.

In the small calorimeter container the crystal and copper-solder can combination was supported by a nylon thread attached to a hole in the pipe used for evacuation of the can. The evacuation pipes were used to connect the calorimeter containers to the external pumping system. Leads from the heater and thermistor were connected to a small array of eight prongs, which in turn were connected to the external measuring apparatus by manganin wire wrapped in teflon tubing extending through the length of the evacuation tube. Note that in Figure 10 the ends of all the evacuation pipes were closed off and that only two small holes on either side of each tube were used for evacuation of the calorimeter chambers. This served the purpose of providing radiation shields to the calorimeter proper.

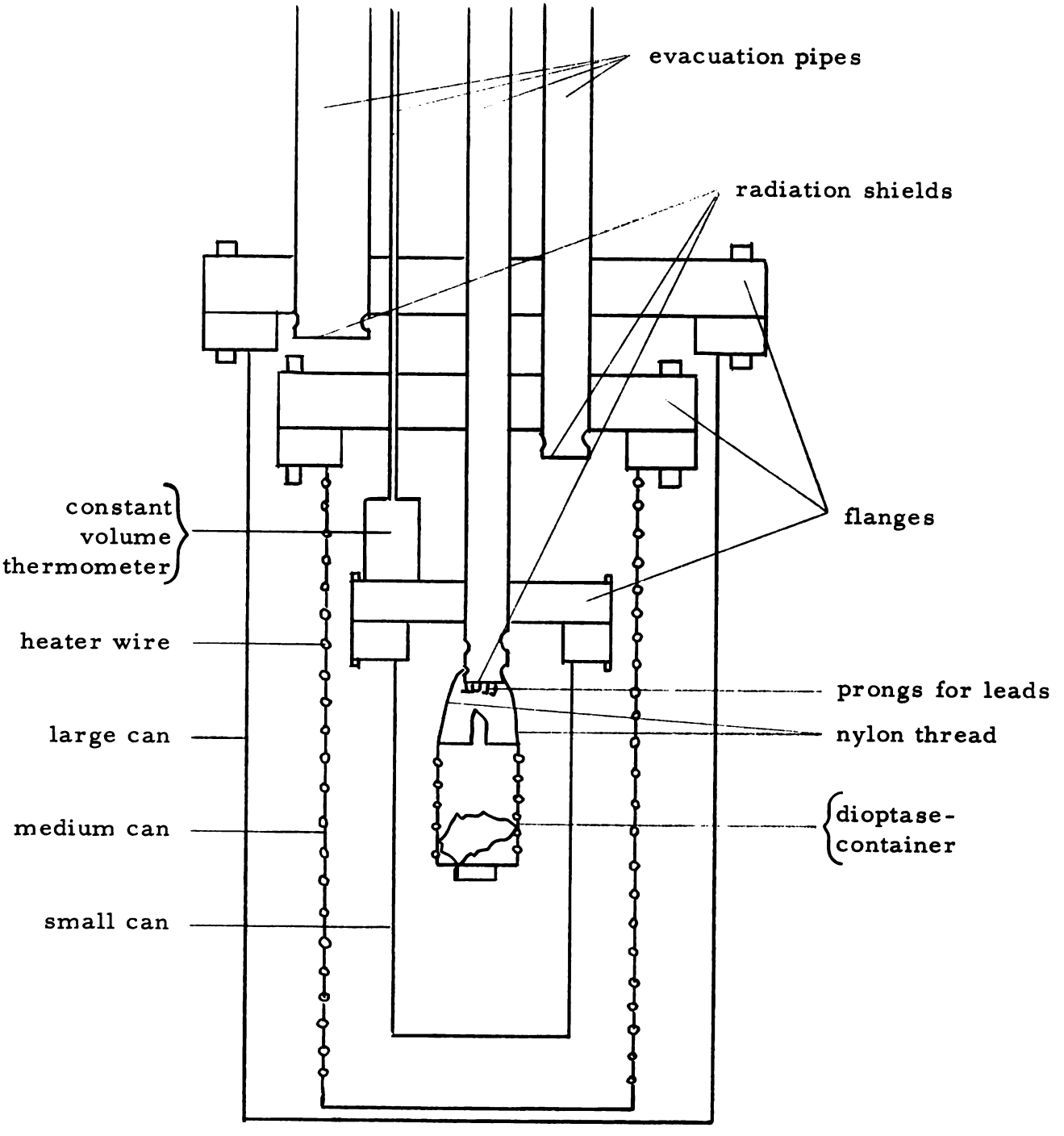

FIGURE 10. Three part calorimeter.

For measurement in the liquid helium temperature range the small can alone would be sufficient; it would act as an adiabatic wall between the crystal and helium bath. In going above 4.2°K, however, it was necessary to use some device to make it "appear to the crystal" that the helium bath in which the entire calorimeter rested (as discussed under "Dewar System") was capable of going to temperatures as high as 70° K. This was accomplished by introduction of a central can cut with fine grooves into which was wound 1500 ohms of manganin wire. By introducing an alternating current of varying effective voltages into the central can it was possible to put in large amounts of heat. From the heat produced by this method in conjunction with the liquid helium background, it was possible to produce temperatures, as seen by the crystal, from 1.2°K to 70°K.

The small and medium cans were then enclosed in a large can. The large can served as an adiabatic wall insulating the heater of the medium can from the helium bath.

All three cans were sealed to their respective flanges by three ampere fuse wire "0"-rings. The leads throughout the calorimeter were brought up through the evacuation pipes to connect to small brass flanges containing glass seals with metal contacts. Connections to the external measuring apparatus were then made from the flanges. An ionization gauge was placed at the top of the evacuation pipes to indicate pressures in the calorimeter system. A constant volume gas

thermometer placed in the calorimeter was to be used as a means of accurately determining temperatures; experimental difficulties were encountered with the gas thermometer, and it was therefore not used.

Dewar System.

The calorimeter was placed in the inner part of a two container dewar arrangement as shown in Figure 11. The outer dewar was used to pre-cool the inner dewar before introduction of the liquid helium. The jacket of the outer dewar was constructed with a permanent vacuum. This prevented heat from entering the liquid air. The jacket of the inner dewar was constructed with a glass stopcock. This permitted frequent pumping on the jacket to eliminate helium gas which diffused into it. The dewars were also silvered to prevent heat loss. A small slit along the side of each dewar allowed observation of the liquid helium and liquid air levels; illumination of the liquids was obtained by a fluorescent light aligned along the slits. The inner dewar was constructed to be leak tight when the calorimeter was placed in it thus allowing the temperature of the liquid helium to be lowered by pumping. A manometer was connected into the pumping line so as to be able to calibrate the thermistor of the crystal-can against the vapor pressure of the liquid helium. The liquid helium was produced in a Collins Helium Cryostat in the laboratory.

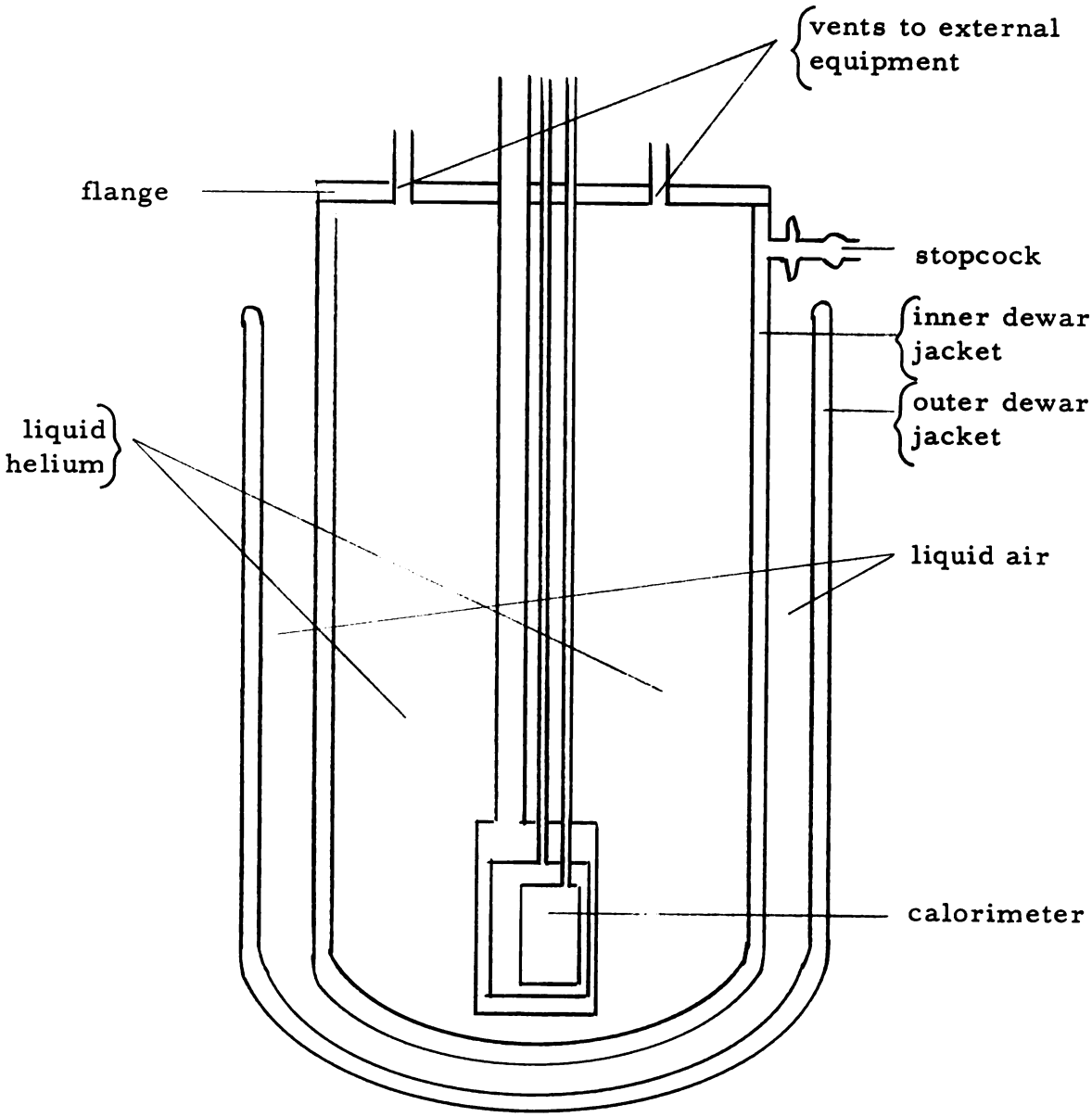

FIGURE 11. Double dewar system.

External Measuring Apparatus.

Three basic circuits were set up for measuring the heat capacities. The first was used for putting heat of known amounts into the crystal. This consisted of a potentiometer, two precision resistors, a galvanometer, a helipot, an electric clock, an ammeter, and other associated equipment. The basic circuit is shown in Figure 12. The potentiometer was connected so as to allow measurement of the voltage V across the heater of the crystal-can suspended in the small colorimeter container. The potentiometer was used also to read the voltage across the precision resistor connected within the heater circuit. The latter reading allowed the heater current I to be determined. A 10 ohm precision resistor was used to determine current values at higher temperatures (above $15^{o}K$) while a 100 ohm resistor was used at lower temperatures. This was done so as to allow the best sensitivity of the potentiometer in the current range being measured. A timer was automatically turned on and off at the same instant a switch controlling the heater current was turned on and off. This gave the time t that the power was put into the heater wire. The heat ΔQ was computed from the relation $\Delta Q = VIt$.

The second circuit was that in which a continuous record of the resistance values of the thermistor was kept. The circuit consisted of two potentiometers, a D. C. Microvolt Amplifier, a Speedomax recorder, a D'Arsonval galvanometer, a microammeter, a helipot,

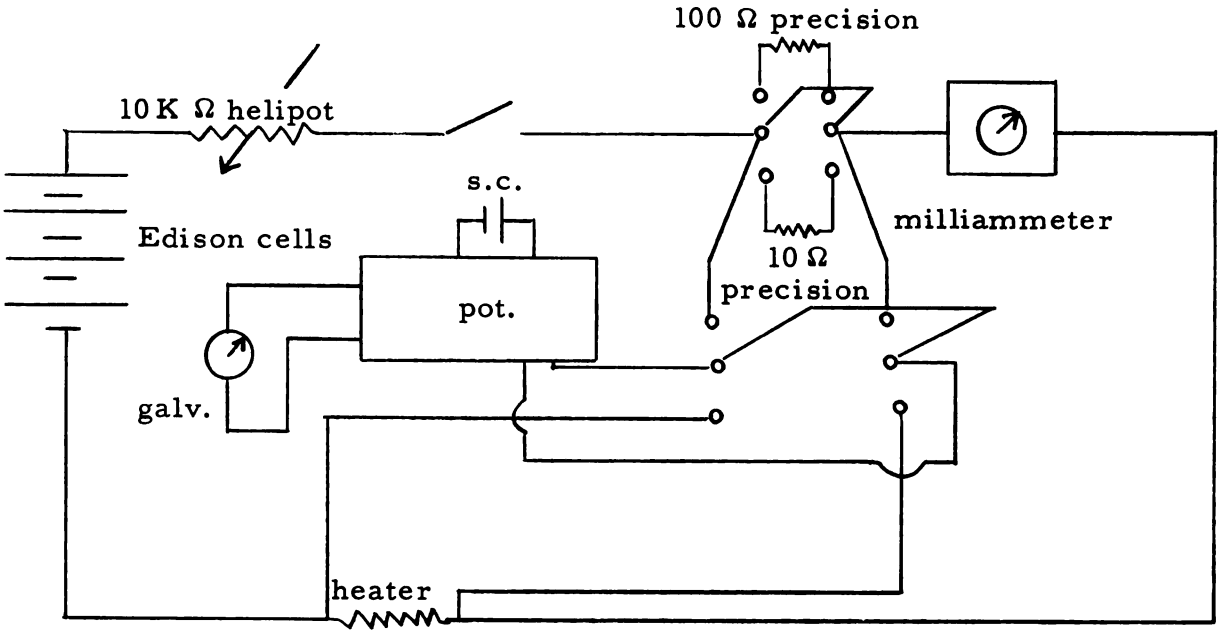

FIGURE 12. Heater circuit.

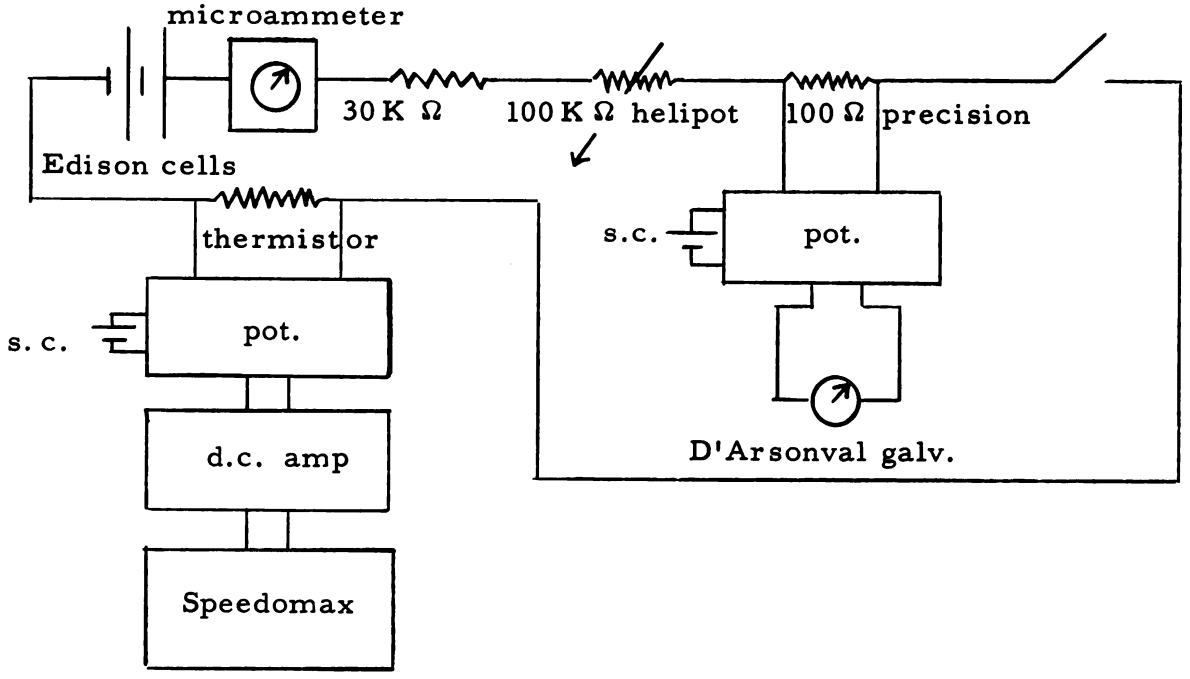

FIGURE 13. Thermometer circuit.

a precision resistor, and other related accessories. By appropriately calibrating the chart of the Speedomax recorder, it was possible to determine the temperature change of the crystal-can when power was put into the heater. The results thus obtained in a single run gave a value of the specific heat at about 80 points at different temperatures. It should be pointed out here that what was actually being measured was the mean specific heat and that the temperatures at which the various heat capacities were found were really average temperatures computed over a small temperature interval. This was carefully taken into account when evaluating the data. A diagram of the thermistor circuit is shown in Figure 13.

To put varying amounts of heat through the heater of the middle can entailed the use of a third circuit. This consisted of an a.c. source, a Variac for course control, and a helipot for fine control. The range of the Variac was from 0 to 110 volts; the helipot had a maximum resistance of 100,000 ohms.

Procedure for Making a Run.

Six basic steps were followed in making a run on the specific heats of the dioptase-can and the can by itself.

1. Assembly: The crystal-can and calorimeter were wired and sealed respectively.
2. Pre-cooling: The inner dewar was evacuated and then filled

with helium exchange gas; liquid air was added to the outer dewar. The system was kept filled with liquid air for at least two to three days.

3. Transferring: The calorimeter was evacuated and then filled with helium exchange gas at 1 mm Hg pressure. Liquid helium was transferred from storage tanks into the inner dewar.

4. Calibration: The thermistor was calibrated against a vapor pressure curve of helium.

5. Evacuation and Measurement: The calorimeter was totally evacuated to about 3×10^{-5} mm Hg and heat capacity measurements made.

6. Warmup: Having gotten the necessary data, the remaining helium was pumped out of the dewar and the liquid air was allowed to boil off. The calorimeter was then removed for disassembly.

The data obtained in Step 4 was used to calibrate the thermistor by use of the equation

$$\left(\frac{\log_{10} R}{T}\right)^{1/2} = a + b \log_{10} R. \qquad (32)$$

That is, the vapor pressure values at various known resistances were converted to temperature values at these resistances.[22] The values so obtained were inserted into Equation (32). Thus "a" and "b," two

unknowns characteristic of the particular carbon resistance being used, were evaluated. "a" was a function of temperature while "b" was constant. The helium vapor pressure method could only be used up to the boiling point of liquid helium ($4.2^{\circ}K$). To obtain values of "a" above this it was necessary to extrapolate the calibration curve to a resistance value corresponding to some known temperature. This was done by measuring the resistance while Step 2 was in progress. This gave the thermistor resistance at liquid nitrogen temperatures, taken to be $77.4^{\circ}K$.

Solving for Equation (32) for T gives

$$T = \frac{\log R}{(a + b \log R)^2} \tag{33}$$

In Step 5 it was merely necessary to compute resistance values on the Speedomax recorder before and after putting heat into the crystal can. Insertion into Equation (33) for the two instances yielded the temperature change ΔT.

RESULTS

The Dioptase Specific Heat Curve.

Three runs were made on the dioptase-container combination and one run was made on the container by itself. Figure 14 shows the results obtained in each dioptase-container run. Figure 15 shows the three dioptase-container runs superimposed. In Figure 15 the data obtained from Run 3 was plotted 1.6°K higher than is shown in Figure 14. This was necessary as the entire curve obtained in Run 3 appeared to be shifted to the left of Runs 1 and 2 by 1.6°K (as explained under "Analysis"). Also plotted in Figure 15 is the data obtained on the copper container run. Graphical subtraction of the container heat capacity values from the dioptase-container values gives the heat capacity of the dioptase crystal; the result is shown in Figure 16. The heat capacity values are given on the ordinate at the left and the converted values to specific heat capacities are shown at the ordinate on the right side of the graph. The actual data obtained from all the runs is given in the Appendix.

Analysis.

Evidence appears in Figure 16 for an anomaly in the heat capacity of the dioptase crystal. This anomaly can also be observed in the plot of the separate runs in Figure 15. A magnetic transition is evident at about 21°K with an uncertainty of ± 2°K. The uncertainty in the

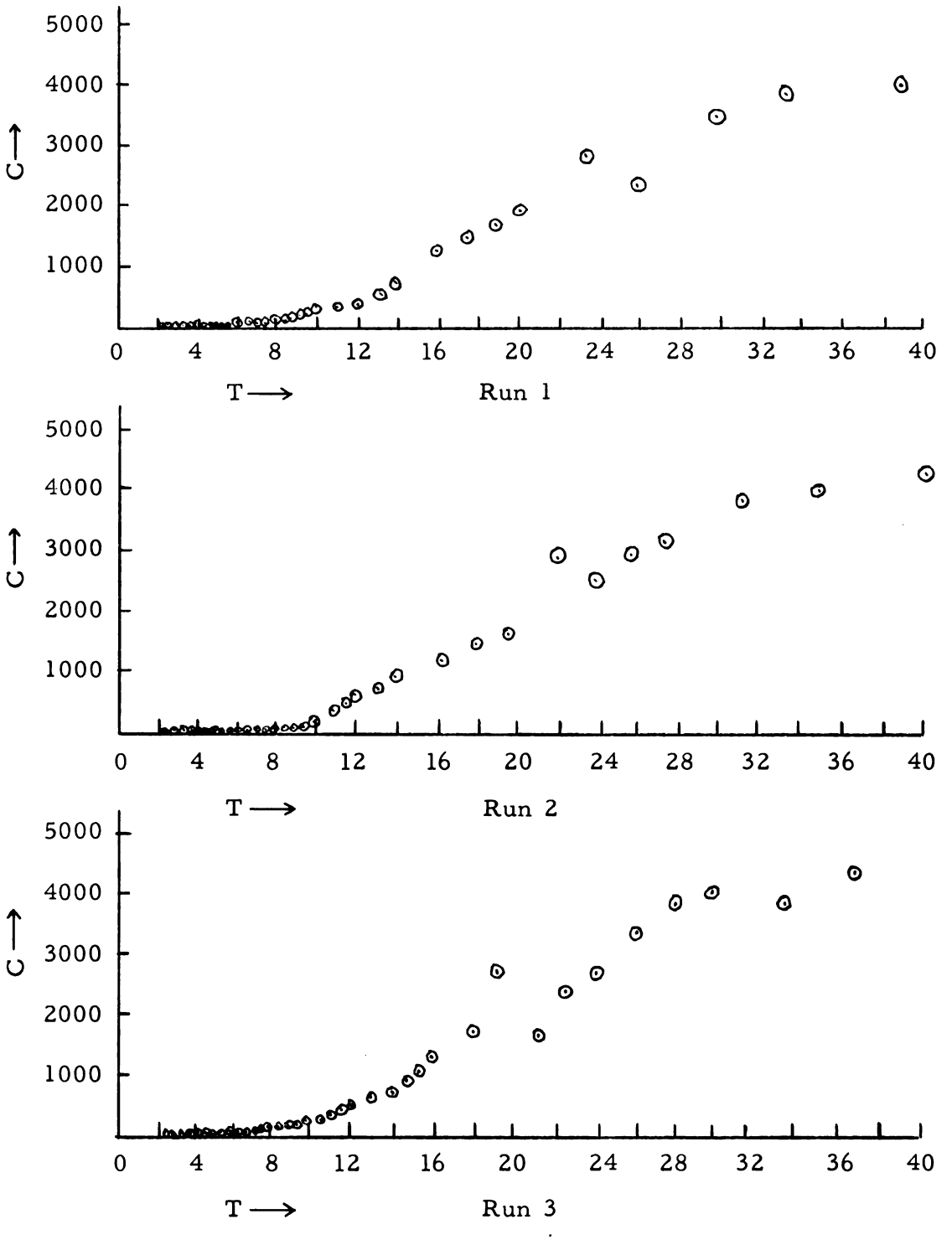

FIGURE 14. Heat capacity (mj/°K) vs. temperature (°K) of dioptase-container combination.

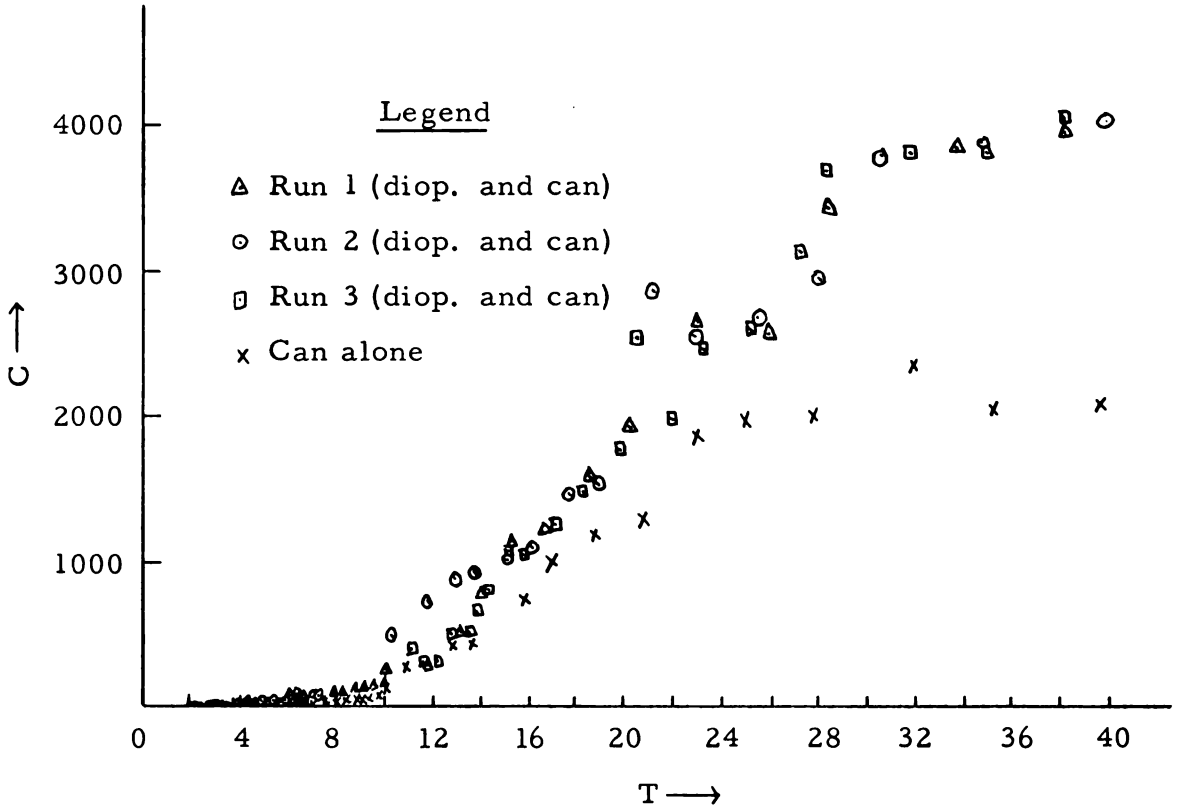

FIGURE 15. Heat capacity (mj/^{o}K) vs. temperature (^{o}K) of all runs on dioptase and container.

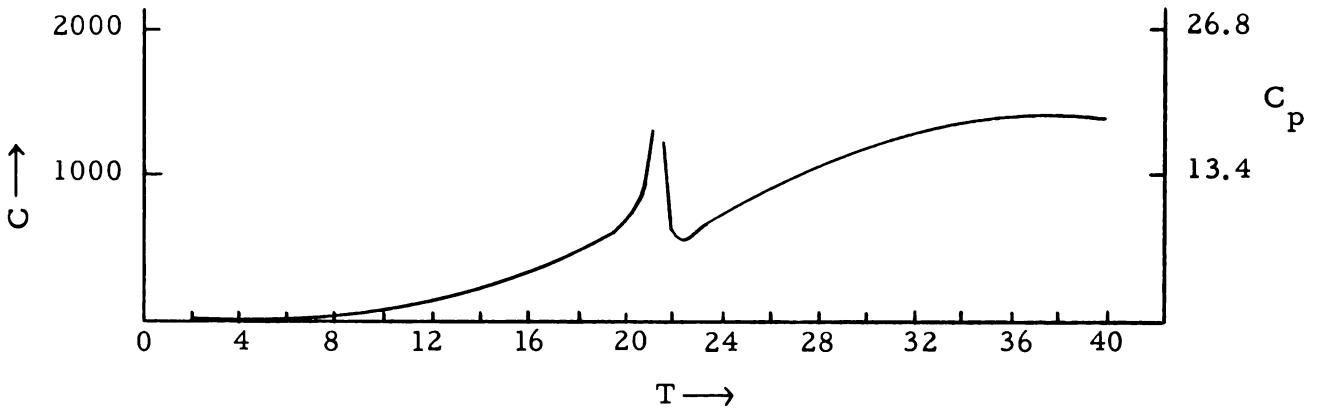

FIGURE 16. Heat capacity (mj/^{o}K) and specific heat capacity (cal/mole ^{o}K) vs. temperature (^{o}K) of dioptase crystal.

temperature is due to the method of calibrating the thermistor. Temperatures were known to an accuracy of $\pm 0.001^{\circ}K$ from $2^{\circ}K$ to $4.2^{\circ}K$ and of $\pm 0.1^{\circ}K$ at liquid nitrogen temperatures ($77.4^{\circ}K$). Between $4.2^{\circ}K$ and $77.4^{\circ}K$, however, the thermistor temperature values were obtained only by interpolation. This uncertainty in temperature measurement probably accounts for the apparent shifting of the data of Run 3 from the data of Runs 1 and 2.

The curves in general follow a Debye T^3 form excepting the region at which the magnetic transition occurs. Above $32^{\circ}K$ the dioptase curve (Figure 16) appears to flatten out and then begin to dip down. This may be due to a Schottky effect, but no generalizations should be made at this part of the curve, however, as there is not sufficient data at the higher temperatures to provide more concrete information. In this region, as well, long equilibrium times were observed which might suggest insensitivity of the thermistor.

An analysis of Figure 16 was made to find the entropy contributions above and below the transition temperature as discussed previously under "Entropy Considerations." In Figure 17 a plot of Equation (29) is shown for the dioptase crystal above $21^{\circ}K$, the data being obtained from Figure 16. In the neighborhood of $21^{\circ}K$ there is a sharp break from linearity. This indicates the points at which Equation (29) is no longer valid. The intercept in Figure 17 gives the value of γ and is found to be about 20 cal $\cdot\, ^{\circ}K$/mole. Since $T_N = 21^{\circ}K$ and $\gamma = 20$ cal $\cdot\, ^{\circ}K$/mole, Equation (30)

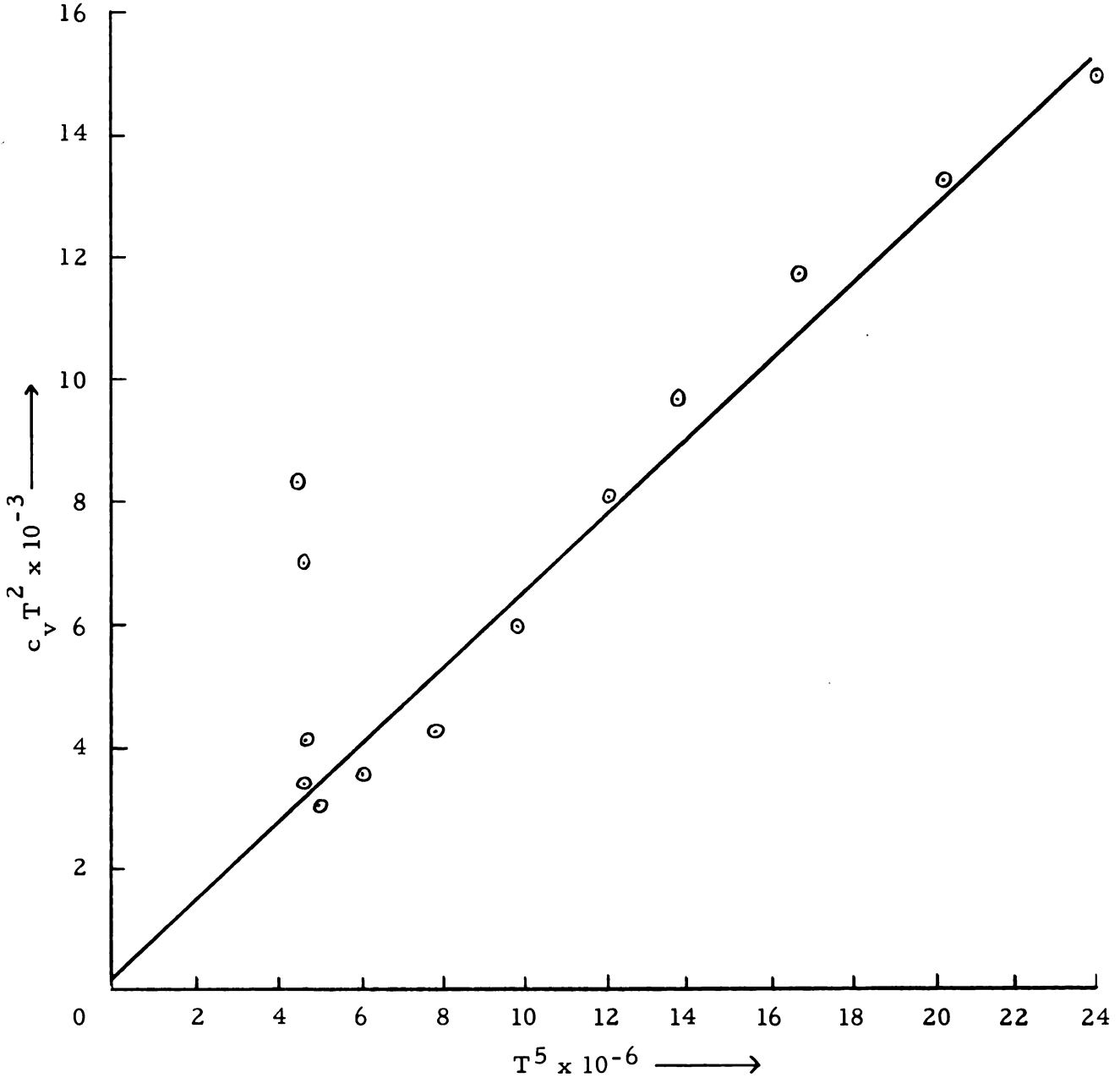

FIGURE 17. Plot of $c_v T^2$ (cal $^\circ$K/mole) vs. T^5 ($^\circ$K)^5 for dioptase above 21°K.

gives the magnetic contribution to the entropy in the paramagnetic state. The value is found to be 0.02 cal/mole $\cdot$ ^{o}K.

Using a graphical method to find the entropy contribution from the antiferromagnetic state, it is first necessary, as previously explained, to subtract the lattice T^3 contribution from the curve of Figure 16. The lattice contribution can be gotten by use of Equation (16). Here the value of a is found from the slope of the line in Figure 17. Figure 18 shows the dioptase specific heat curve and the lattice contribution. The difference of the curves represents the magnetic contribution to the specific heat (C_{mag}). Plotting C_{mag}/T vs. T and measuring the area, the entropy due to the antiferromagnetic state of the dioptase is found. The value so obtained is 1.17 cal/mole ^{o}K.

Using Equation (31) and noting that $s = 1/2$ for the Cu^{++} ion in $CuSiO_3 \cdot H_2O$, the theoretical value for the total magnetic contribution to the entropy is $S_{tot} = 1.39$ cal/mole $\cdot$ ^{o}K. Experimentally $S_{tot} = S_{para} + S_{antifer} = 0.02 + 1.17 = 1.19$ cal/mole $\cdot$ ^{o}K, a result in good agreement with theory. The antiferromagnetic entropy contribution is about 98%, while the paramagnetic contribution is about 2%, due probably to short range ordering.

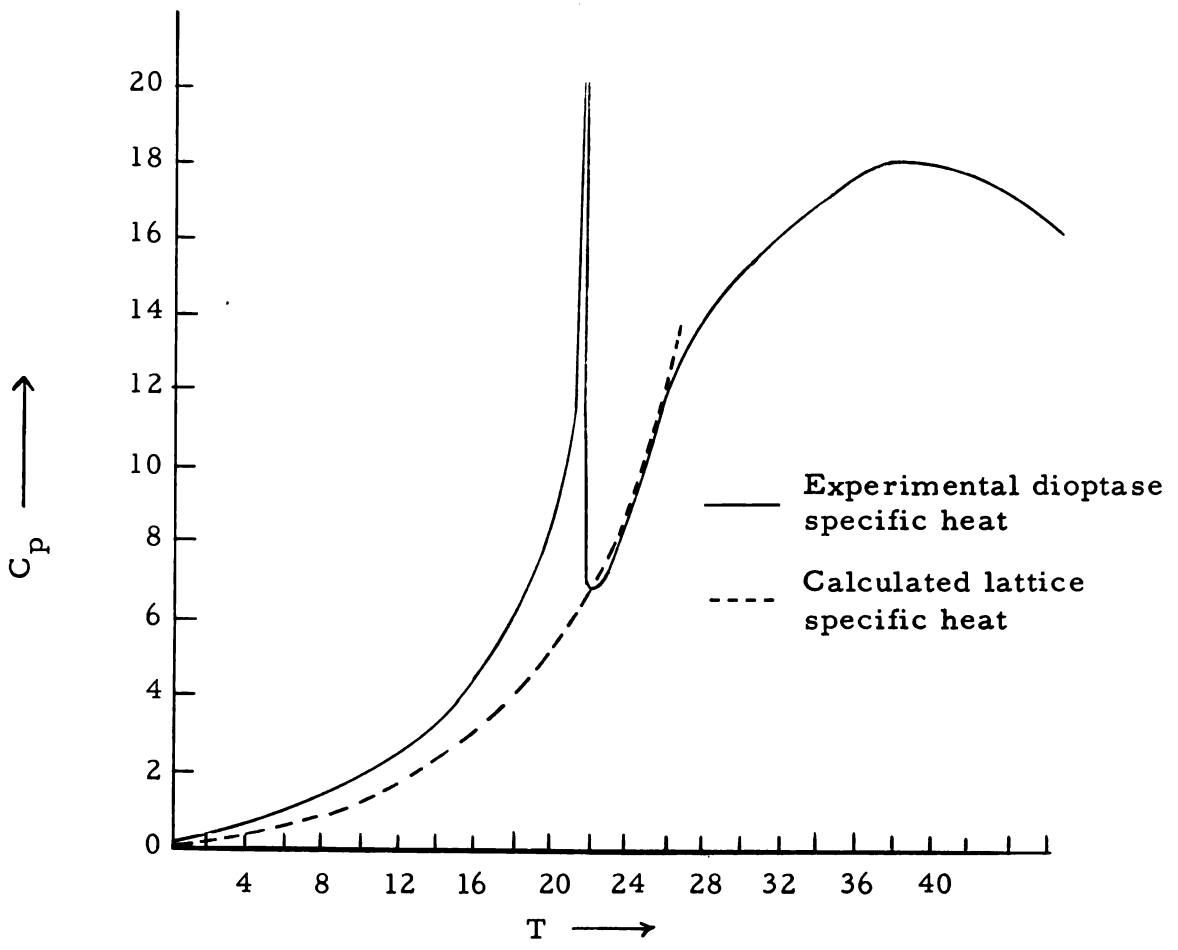

FIGURE 18. Specific heat (cal/mole · °K) vs. temperature (°K) for experimental dioptase data and calculated lattice contribution.

REFERENCES

1. F. W. Sears, Thermodynamics (Addison-Wesley Pub. Co., Cambridge, Mass., 1956).
2. D. H. Parkinson, Rep. Progr. Phys., 21, 226 (1958).
3. L. V. Azaroff, Introduction to Solids (McGraw-Hill Book Co., Inc., New York, 1960).
4. P. Drude, Ann. Physik, 1, 566 (1900).
5. C. Kittel, Introduction to Solid State Physics (John Wiley and Sons, Inc., New York: 2nd edition, 1956).
6. C. G. Maier and C. T. Anderson, J. Chem. Phys., 2, 513 (1934).
7. A. Einstein, Ann. Physik, 22, 180 (1906).
8. F. Seitz, Modern Theory of Solids (McGraw-Hill Book Co., Inc., New York, 1940).
9. P. Debye, Ann. Physik, 39, 789 (1912).
10. R. D. Spence, H. Forstat, G. A. Khan, and G. Taylor, J. Chem. Phys., 31, 555 (1959).
11. J. H. Van Vleck, J. Chem. Phys., 5, 320 (1937).
12. J. H. Van Vleck, J. Chem. Phys., 9, 85 (1941).
13. C. J. Gorter, Revs. Modern Phys., 25, 332 (1953).
14. Bizette, Squire, and Tsai, Compt. Rend., 207, 449 (1938).
15. A. B. Lidiard, Rep. Progr. Phys., 17, 201 (1954).

16. Ibid.

17. S. A. Friedberg, Physica, 18, 714 (1952).

18. D. G. Kapadnis and R. Hartman, Physica, 22, 181 (1956).

19. J. R. Clement and E. H. Quinnel, Rev. Sci. Instr., 23, 213 (1952).

20. G. O. Taylor, Jr., "Low Temperature Heat Capacities of Single Crystals" (unpublished Master's thesis, Dept. of Physics and Astronomy, Michigan State University, 1960).

21. R. D. Spence and J. H. Muller, J. Chem. Phys., 29, 961 (1958).

22. F. G. Brickwedde, J. Research of National Bureau of Standards, 64A, 1 (1960).

APPENDIX

Experimental Data Obtained from All Runs

First Run on Dioptase-Container, August 2, 1963.

$\bar{T}$ (°K)	ΔT (°K)	C (mj/°K)	$\bar{T}$ (°K)	ΔT (°K)	C (mj/°K)
2.19	0.0010	37	3.99	0.013	44
2.21	0.0007	55	4.10	0.015	45
2.23	0.0011	32	4.29	0.022	31
2.25	0.0011	32	4.47	0.024	37
2.27	0.0010	34	4.68	0.060	16
2.32	0.0014	26	5.02	0.042	20
2.34	0.0011	33	5.27	0.024	37
2.38	0.0011	36	5.46	0.017	56
2.41	0.0008	45	5.67	0.033	30
2.44	0.0008	44	5.97	0.020	45
2.47	0.0010	36	6.26	0.021	53
2.50	0.0019	37	6.54	0.033	61
2.54	0.0016	36	6.78	0.023	83
2.57	0.0016	31	6.96	0.023	80
2.61	0.0018	30	7.16	0.035	75
2.65	0.0016	36	7.68	0.030	90
2.69	0.0012	44	8.15	0.024	100
2.74	0.0024	42	8.60	0.027	140
2.83	0.0027	26	9.08	0.024	200
2.86	0.0022	35	9.49	0.040	250
2.90	0.0043	36	9.85	0.039	260
2.95	0.0025	38	10.4	0.095	210
3.00	0.0020	47	11.9	0.086	270
3.05	0.0035	26	13.2	0.050	480
3.09	0.0042	38	14.5	0.050	790
3.15	0.0043	42	15.5	0.10	1100
3.20	0.0037	45	17.1	0.48	1200
3.26	0.0068	29	19.0	0.30	1600
3.33	0.0050	39	20.8	0.26	1900
3.40	0.011	22	23.6	0.26	2700
3.49	0.0054	36	26.2	0.42	2500
3.58	0.010	27	29.4	0.53	3400
3.67	0.0075	34	33.8	0.71	3800
3.76	0.0090	47	38.8	1.0	4000
3.85	0.010	38			

Second Run on Dioptase-Container, August 6, 1963.

$\bar{T}$	ΔT	C	$\bar{T}$	ΔT	C
2. 28	0. 0024	28	5. 22	0. 040	30
2. 30	0. 0027	26	5. 43	0. 028	46
2. 33	0. 0020	29	5. 66	0. 025	34
2. 36	0. 0015	35	5. 98	0. 024	50
2. 39	0. 0022	33	6. 22	0. 033	50
2. 42	0. 0021	39	6. 45	0. 020	59
2. 46	0. 0024	32	6. 77	0. 026	58
2. 49	0. 0021	34	7. 07	0. 025	77
2. 53	0. 0017	41	7. 40	0. 029	92
2. 56	0. 0016	47	7. 65	0. 025	110
2. 60	0. 0023	32	7. 87	0. 032	120
2. 64	0. 0027	36	8. 17	0. 038	130
2. 67	0. 0025	34	8. 51	0. 037	140
2. 71	0. 0021	43	8. 87	0. 041	190
2. 96	0. 0043	44	9. 24	0. 052	160
3. 01	0. 0021	72	9. 60	0. 050	250
3. 05	0. 0049	47	9. 98	0. 060	270
3. 10	0. 0033	53	10. 5	0. 081	370
3. 14	0. 0042	52	11. 3	0. 12	470
3. 19	0. 0047	53	12. 0	0. 064	700
3. 25	0. 0025	73	12. 7	0. 25	190
3. 30	0. 0038	70	13. 3	0. 11	840
3. 36	0. 0041	59	14. 1	0. 095	900
3. 40	0. 0043	51	15. 1	0. 22	990
3. 45	0. 0040	55	16. 6	0. 22	1100
3. 51	0. 0034	58	18. 1	0. 21	1400
3. 58	0. 0057	65	19. 7	0. 25	1500
3. 64	0. 0032	90	21. 4	0. 21	2800
4. 21	0. 017	42	23. 6	0. 34	2500
4. 31	0. 012	52	25. 8	0. 46	2700
4. 47	0. 020	30	28. 3	0. 66	3100
4. 59	0. 012	47	31. 3	0. 75	3800
4. 69	0. 014	41	35. 3	1. 1	3700
4. 81	0. 017	32	40. 3	1. 7	4000

Third Run on Dioptase-Container, August 7, 1963.

$\bar{T}$	ΔT	C	$\bar{T}$	ΔT	C
2.27	0.0023	23	4.26	0.0068	56
2.29	0.0023	42	4.36	0.016	31
2.31	0.0033	33	4.45	0.015	32
2.34	0.0022	33	4.55	0.019	36
2.37	0.0018	41	4.65	0.012	46
2.40	0.0019	38	4.74	0.022	24
2.42	0.0020	39	4.86	0.015	35
2.45	0.0022	33	5.25	0.020	39
2.48	0.0016	46	5.42	0.021	36
2.50	0.0012	61	5.58	0.031	30
2.54	0.0021	36	5.79	0.026	36
2.57	0.0023	38	6.01	0.032	31
2.64	0.0025	33	6.21	0.022	44
2.68	0.0023	36	6.43	0.024	48
2.71	0.0029	29	6.86	0.025	99
2.75	0.0029	30	7.05	0.033	83
2.80	0.0027	31	7.21	0.023	89
2.87	0.0037	32	7.39	0.026	100
2.91	0.0024	41	7.55	0.031	80
2.95	0.0034	50	7.85	0.0090	310
2.99	0.0040	41	8.20	0.013	260
3.03	0.0029	44	8.56	0.034	130
3.06	0.0031	43	8.93	0.037	160
3.10	0.0041	45	9.27	0.054	200
3.14	0.0030	58	9.61	0.073	120
3.26	0.0043	40	9.91	0.030	390
3.32	0.0088	32	10.2	0.064	290
3.38	0.0047	46	10.6	0.048	330
3.44	0.0079	28	11.3	0.055	510
3.49	0.0046	47	11.9	0.10	470
3.55	0.0095	23	12.5	0.096	650
3.62	0.0085	40	13.1	0.16	780
3.68	0.020	13	13.8	0.20	1000
3.75	0.0080	33	14.7	0.20	1000
3.82	0.013	30	15.8	0.25	1300
3.95	0.0054	65	17.0	0.26	1300
4.01	0.014	31	18.3	0.22	1700

(continued)

$\bar{T}$	ΔT	C	$\bar{T}$	ΔT	C
4.10	0.0064	64	19.4	0.17	2500
4.18	0.012	32	20.7	0.28	1900
22.2	0.33	2400	30.4	0.58	3800
23.9	0.35	2600	33.6	0.79	3800
25.8	0.27	3300	27.1	0.96	4100
27.8	0.43	3900			

Run on Container Alone, August 13, 1963.

$\bar{T}$	ΔT	C	$\bar{T}$	ΔT	C
2.29	0.004	51	3.87	0.0061	39
2.31	0.0014	34	3.92	0.0072	32
2.34	0.0013	33	3.97	0.0056	43
2.36	0.0013	33	4.03	0.0044	52
2.38	0.0020	34	4.08	0.0057	47
2.41	0.0026	41	4.13	0.0048	51
2.47	0.0019	33	4.19	0.0065	52
2.49	0.0018	35	4.32	0.0064	43
2.53	0.0018	36	4.46	0.015	24
2.56	0.0017	37	4.60	0.013	31
2.59	0.0013	50	4.70	0.0098	33
2.63	0.0013	49	4.79	0.015	22
2.66	0.0017	37	4.97	0.014	30
2.69	0.0024	34	5.12	0.012	33
2.73	0.0028	26	5.21	0.013	30
2.76	0.0024	25	5.36	0.014	28
2.80	0.0018	30	5.48	0.014	28
2.83	0.0019	39	5.60	0.019	27
2.87	0.0027	34	5.76	0.022	22
2.90	0.0022	40	5.96	0.024	22
2.94	0.0018	49	6.33	0.022	34
2.97	0.0021	42	6.49	0.020	58
3.01	0.0023	38	6.72	0.021	41
3.04	0.0024	43	6.92	0.024	56
3.08	0.0020	52	7.12	0.031	51
3.11	0.0021	46	7.32	0.029	59
3.15	0.0021	46	7.50	0.037	65
3.22	0.0058	20	7.72	0.036	68

(continued)

$\bar{T}$	ΔT	C	$\bar{T}$	ΔT	C
3.58	0.0030	57	7.99	0.048	69
3.67	0.0046	43	8.28	0.034	97
3.72	0.0043	52	8.56	0.048	97
3.76	0.0034	53	8.95	0.11	120
3.82	0.0058	52	9.38	0.052	150
9.77	0.058	150	18.9	0.47	1100
10.7	0.054	190	21.1	0.24	1200
11.2	0.048	320	23.3	0.19	1900
11.8	0.070	320	25.5	0.27	1900
12.5	0.14	260	28.3	0.45	1800
13.4	0.19	400	31.7	0.57	2600
14.5	0.14	440	35.7	1.4	2100
15.7	0.092	680	46.5	1.2	2700
17.0	0.11	1000			